Reductive Dehalogenation of Trichloroethylene with Zero-Valent Iron: Surface Profiling Microscopy and Rate Enhancement Studies

J. Gotpagar,[†] S. Lyuksyutov,[‡] R. Cohn,[‡] E. Grulke,[†] and D. Bhattacharyya*[,†]

Department of Chemical and Materials Engineering, University of Kentucky, Lexington, Kentucky 40506, and The Electrooptics Research Institute, University of Louisville, Louisville, Kentucky 40292

Received March 18, 1999. In Final Form: July 9, 1999

Mechanistic aspects of the reductive dehalogenation of trichloroethylene using zerovalent iron are studied with three different surface characterization techniques. These include scanning electron microscopy, surface profilometry, and atomic force microscopy. It was found that the pretreatment of an iron surface by chloride ions causes enhancement in the initial degradation rates. This enhancement was attributed to the increased roughness of the iron surface due to crevice corrosion obtained by pretreatment. The results indicate that the "fractional active site concentration" for the reactive sorption of trichloroethylene is related to the number of defects/abnormalities present on the surface of the iron. This was elucidated with the help of atomic force microscopy. Two possible mechanisms include (1) a direct hydrogenation in the presence of defects acting as catalyst and (2) an enhancement due to the two electrochemical cells operating in proximity to each other. The result of this study has potential for further research to achieve an increase in the reaction rates by surface modifications in a practical scenario.

1. Introduction

Since the original studies by Gillham and O'Hannesin[1,2] who proposed the use of reductive dehalogenation reaction for environmental remediation, several studies have been published which deal with the reaction of trichloroethylene (TCE) with zerovalent iron. Matheson and Tratnyek[3] were the first to report a detailed kinetic and mechanistic study of this reaction with several contaminants of concern. It is well-known now that though these reactions are faster compared to the natural biotic and abiotic processes, the rates are nonetheless too low to be feasible for ex situ applications. Therefore, the focus so far in this area is directed toward the in situ applications. Both in situ reactive barriers and above ground reactors have been developed for this purpose. Several test installations have already been completed at contaminated sites, and more are being planned.[4−7] However, little information is available on the exact mechanism of the reductive dehalogenation using zerovalent iron. The effective design and operation of systems involving zerovalent metals would be greatly improved by a more detailed, process-level understanding of the mechanism by which these contaminants degrade. Furthermore, improving the rates of these processes would also make the ex situ applications feasible and reduce the remediation time and would also be cost-effective. In this paper, an attempt is made to gain an understanding of the surface phenomena on the surface of iron during the reductive dehalogenation of TCE with the ultimate goal of increasing the rate of reaction. Atomic force microscopy (AFM), surface profilometry, and scanning electron microscopy (SEM) were used to analyze the surface features of the iron. In addition, the relation between the metal dissolution process occurring during dehalogenation of chlorinated organics to the classical crevice corrosion mechanism of iron in the presence of chloride ion is described. Only recently, promising use of AFM was suggested by Boronina et al.[8] for such environmental applications. In this study, AFM is also found to be important for the indication of crevice corrosion, as will be discussed later on.

2. Background. Role of the Metallic Surface

2.1. Role of the Metal Surface on Electron Transfer. Although considerable advancement has been made recently in identifying the product distribution,[9−11] to date the exact surface mechanism for TCE degradation by iron is not known. There is general agreement that electron transfer at the metal surface is required. This observation was used by Gotpagar et al.[12] and Boronina et al.[13] to develop the macroscopic model. Recent publications[3,5,13−18] have repeatedly emphasized the importance of the metal

* To whom correspondence should be addressed. Phone: (606) 257-2794. Fax: (606) 323-1929. E-mail: db@engr.uky.edu.

[†] University of Kentucky.

[‡] University of Louisville.

(1) Gillham, R. W.; O'Hannesin, S. F. Metal-catalyzed Abiotic Degradation of Halogenated Organic Compounds. Paper presented at the 1992 IAH Conference on Modern Trends in Hydrogeology, Hamilton, Ontario, Canada, May 10−13, 1992.

(2) Gillham, R. W.; O'Hannesin, S. F. *Groundwater* **1994**, *32*, 958.

(3) Matheson, L. J.; Tratnyek, P. G. *Environ. Sci. Technol.* **1994**, *28*, 2045.

(4) Gillham, R. W.; O'Hannesin, S. F.; Orth, W. S. Metal Enhanced Abiotic 5. Degradation of Halogenated Aliphatics: Laboratory Tests and Field Trials. Paper presented at the 1993 HazMat Central Conference, Chicago, IL, March 9−11, 1993.

(5) Gillham, R. W. *Prepr. Extended Abstr. Am. Chem. Soc.* **1995**, *35*, 691.

(6) Puls, R. W.; Powell, R. M. *Environ. Sci. Technol.* **1997**, *31*, 2244.

(7) Yamane, C. L.; Gallinatti, J. D.; Szerdy, F. S.; Delfino, T. A.; Hankins, D. A.; Vogan, J. L. *Prepr. Extended Abstr. Am. Chem. Soc.* **1995**, *35*, 792.

(8) Boronina, T. N.; Lagadic, I.; Sergeev, G. B.; Klabunde, K. J. *Environ. Sci. Technol.* **1998**, *32*, 2614.

(9) Roberts, A. L.; Wells, J. R.; Campbell, T. J.; Burris, D. R. *Environ. Toxicol. Chem.* **1997**, *16*, 625.

(10) Burris, D. R.; Delcomyn, C. A.; Smith, M. H.; Roberts, A. L. *Environ. Sci. Technol.* **1996**, *30*, 3047.

(11) Arnold, W. A.; Roberts, A. L. *Environ. Sci. Technol.* **1998**, *32*, 3017.

(12) Gotpagar, J.; Grulke, E.; Tsang, T.; Bhattacharyya, D. *Environ. Prog.* **1997**, *16*, 137.

(13) Boronina, T.; Klabunde, K. J.; Sergeev, G. *Environ. Sci. Technol.* **1995**, *29*, 1511.

10.1021/la990325x CCC: $18.00
Published on Web 09/18/1999

surface area in the process. It was also found that the presence of carbonate- or oxide-forming species in the water leads to an inert layer of metal oxide or metal carbonate forming on the metal surface. This layer greatly reduces the overall reaction rate.[18−21] Thus, it is quite clear that the metallic surface is the controlling factor in TCE degradation.

Current research efforts are directed toward obtaining enhancements in reaction rates. Bimetallic complexes have been used to generate higher chlorinated organic degradation rates.[22−25] In particular, Li and Klabunde have shown that doping various zinc samples with palladium, silver, and nickel resulted in much higher pseudo-first-order degradation rates, with some systems showing as much as 150 times higher values. The standard oxidation−reduction potentials of these metals relative to a hydrogen electrode are +0.987 (Pd), +0.799 (Ag), −0.250 (Ni), −0.440 (Fe), and −0.763 (Zn). For each metal pair, the metal with the lower potential is preferentially dissolved, releasing electrons, e.g., the zinc dissolution in the Pd−Zn pair.

When iron is used, the chemistry at the metal surface during a dehalogenation can be similar to that of classical crevice corrosion of steel in the presence of chloride ions.[26] In the presence of oxygen, iron metal is oxidized, releasing electrons, which can be used in the reduction reaction of water plus oxygen, generating hydroxide ions. Depletion of oxygen in crevices leads to an excess of positive charges in the local solution, causing the diffusion of chloride ions into these spaces and increasing the metal dissolution. Insoluble metal hydroxides can form and coat the exterior surface, reducing the rate of metal dissolution.

The presence of a second metal electropositive relative to iron would provide surfaces that might exhibit less fouling and could continue to supply electrons to a complete oxidation−reduction process cycle. Furthermore, the presence of a second, nonreactive metal would accelerate the dissolution of the reactive metal in crevices. This surface area affect would add to the faster chloride ion migration within the crevices. For example, Li and Klabunde[25] showed that more porous zinc was formed during their degradations. In their case, the second electropositive metal could have accelerated the process both by providing a nonfouling surface for reduction reactions and by promoting crevice formation in the zinc-rich areas of the material (enhanced via the chloride ion diffusion process). Surface Fe^{2+} has been shown to play a very important role in the degradation of chlorinated organics.

The decrease in the reaction rate with time for zerovalent iron systems may be due to changes in the iron surface morphology. For example, the formation of insoluble iron hydroxides could foul the surface, reducing the reduction process and slowing the development of crevices. One approach reported in this area was the use of bimetallic complexes.[25] Matheson and Tratnyek[3] have argued that commonly used bimetallic systems include a hydrogenation catalyst such as Ni or Pd that can further enhance the rate. Although the results obtained with such bimetallic systems seem encouraging, the enhanced degradation rates have only been studied for short periods of time. The outer layer of these materials are quickly covered with iron oxides,[22,27,28] thus causing rate reduction.

Another new approach for iron surface (without the use of bimetallic systems) regeneration is the use of ultrasound. This is confirmed by a recently published study,[29] which observed overall rate enhancement by a factor of 40 for dechlorination of CCl_4 by zerovalent iron, in the presence of ultrasound waves. The reason for this enhancement was attributed to the continuous cleaning and activation of the Fe^0 surface by ultrasound waves, and the enhanced rates of mass transport resulting from cavitation. Characterization of the iron surface can thus provide helpful insight into the mechanistic aspects of the reaction, thereby potentially leading to the enhancement of process effectiveness.

2.2. Sorption of TCE onto the Iron Surface. The first step in the reaction of TCE reduction with Fe^0 is the TCE sorption onto the iron surface. The sorption of TCE takes place at two different sites—reactive sites and nonreactive sites. Moreover, Burris et al.[30] have shown that the majority of this sorption takes place at the nonreactive sites. It was shown that the adsorption of TCE to iron follows the modified Langmuir type isotherm given by

$$C^{S}_{TCE} = kb(C^{W}_{TCE})^{M}/(1 + k(C^{W}_{TCE})^{M}) \quad (1)$$

where C^{S}_{TCE} and C^{W}_{TCE} are the sorbed concentration (nmol/g) and aqueous phase concentration (nmol/ml), respectively. M, k, and b are generalized Langmuir coefficients.[30] In our earlier published study,[17] the concept of fractional active site concentration was introduced to take into account this difference in the sorption behavior. The fractional active site concentration was defined as

$$A_S = C^{S*}_{TCE}/C^{S}_{TCE} \quad (2)$$

where A_S is the fractional active site concentration and C^{S*}_{TCE} is the concentration of TCE on reactive sites (nmol/g). It was shown that, with this concept of fractional active site concentration, the model developed was able to predict the degradation of TCE with time quite accurately over the entire course of time. The equation indicating the decline in the concentration of TCE in a simple two-phase

(14) Lipczynska-Kochany, E.; Harms, S.; Milburn, R.; Sprah, G.; Nadarajah, N. *Chemosphere* **1994**, *29*, 1477.
(15) Helland, B. R.; Alvarez, P. J. J.; Schnoor, J. L. *J. Haz. Mater.* **1995**, *41*, 205.
(16) Warren, K. D.; Arnold, R. L.; Bishop, T. L.; Lindholm, L. C.; Betterton, E. A. *J. Haz. Mater.* **1995**, *41*, 217.
(17) Gotpagar, J.; Grulke, E.; Bhattacharyya, D. *J. Haz. Mater.* **1998**, *62*, 243.
(18) MacKenzie, P. D.; Baghel, S. S.; Eykholt, G. R.; Horney, D. P.; Salvo, J. J.; Sivavec, T. M. American Chemical Society Extended Abstract, Industrial and Engineering Chemistry Division, Sept 17−20, 1995, pp 59−62.
(19) Agrawal, A.; Liang, L.; Tratnyek, P. G. American Chemical Society Extended Abstract, Industrial and Engineering Chemistry Division, Sept 17−20, 1995, p 54.
(20) Liang, L.; Goodlaxson, J. D. American Chemical Society Extended Abstract, Industrial and Engineering Chemistry Division, Sept 17−20, 1995, pp 46−49.
(21) Sivavec, T. M.; Horney, D. P.; Baghel, S. S. American Chemical Society Extended Abstract, Industrial and Engineering Chemistry Division, Sept 17−20, 1995, pp 42−45.
(22) Muftikian, R.; Fernando, Q.; Korte, N. *Water Res.* **1995**, *29*, 2434.
(23) Roberts, A. L.; Fennelly, J. P. *Environ. Sci. Technol.* **1988**, *32*, 1980.
(24) Korte, N. E.; Grittini, C.; Muftikian, R.; Fernando, Q.; Liang, L.; Clausen, J. American Chemical Society Extended Abstract, Industrial and Engineering Chemistry Division, Sept 17−20, 1995, pp 51−53.
(25) Li., W.; Klabunde, K. J. *Croat. Chem. Acta* **1998**, *71*, 853.
(26) Fontana, M. G.; Greene, N. D. *Corrosion Engineering*, 2nd ed., McGraw-Hill Book Co.: New York, 1978.
(27) Muftikian, R.; Nebesney, K.; Fernando, Q.; Korte, N. *Environ. Sci. Technol.* **1996**, *30*, 3593.
(28) Sivavec, T. M.; Mackenzie, P. D.; Horney, D. P. American Chemical Society Extended Abstract, Industrial and Engineering Chemistry Division, April 13−17, 1997, pp 83−85.
(29) Hung, H.-M.; Hoffmann, M. R. *Environ. Sci. Technol.* **1998**, *32*, 3011.
(30) Burris, D. R.; Campbell, T. J.; Manoranjan, V. S. *Environ. Sci. Technol.* **1995**, *29*, 2850.

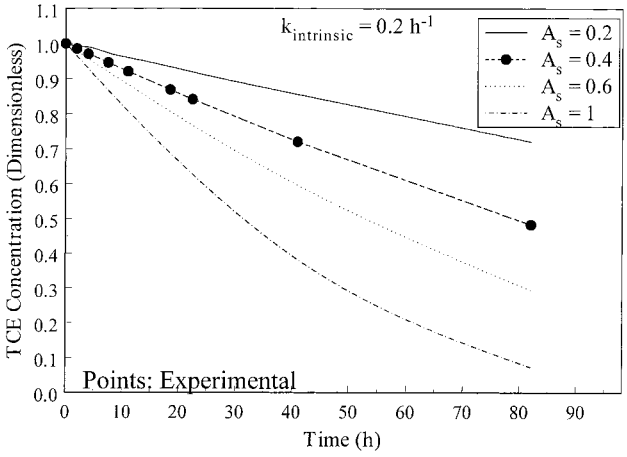

Figure 1. Effect of fractional active site concentration on the simulated TCE degradation profile with zerovalent iron.

(solid−liquid) closed system with iron and TCE dissolved in water was obtained as

$$\frac{dC_{TCE}^{W}}{dt} = -\frac{(kb(C_{TCE}^{W})^{M}/(1 + k(C_{TCE}^{W})^{M}))k_{intrinsic}A_S m_{Fe}}{V^{W}[1 + (m_{Fe}Mkb(C_{TCE}^{W})^{M-1})/(V_W(1 + k(C_{TCE}^{W})^{M})^2)]} \quad (3)$$

where m_{Fe} is the amount of iron used in the reaction system (g), V_W is the volume of the aqueous phase used (L), and $k_{intrinsic}$ is the intrinsic value of the degradation rate constant (h^{-1}). The above equation is also consistent with the observed zero-order reaction behavior at higher TCE concentrations. The result of this modeling analysis[31] indicated that the actual intrinsic degradation constant and the observed value of the same are related by

$$k_{obs} = (kbA_S m_{Fe}/3V_W)k_{intrinsic} \quad (4)$$

where k_{obs} is the observed value of the degradation constant (h^{-1}). It is instructive to note from the above equation that even if the actual intrinsic degradation constant value for the reaction of reductive dehalogenation is high, due to the small coverage of the reactive sites, the overall degradation constant value would be lowered to a great extent (almost an order of magnitude). This is also clear from Figure 1, which shows the effect of fractional active site concentration on the calculated TCE degradation. As expected, increasing the value of A_S causes an increase in the degradation rate. The calculated curve for $A_S = 0.4$ fits the experimental data quite well (with $k = 0.0207$, $b = 882$, and $M = 0.655$, values obtained from Burris et al.[30]). Thus, one should look at different ways to improve the active surface area to explore the possible enhancements in the degradation rates. The role of surface area was further verificated by Li and Klabunde,[25] in which ultrafine zinc coated with small amounts of palladium gave the highest reactivity for carbon tetrachloride dechlorination. As mentioned in the previous section, the oxide layer present on the surface of iron was found to slow the TCE degradation. In other words, the active surface available for the TCE degradation is reduced as time progresses. Continuous cleaning of the surface (increasing A_S) was found to increase the degradation rate considerably.[29]

It is clear that the low rates of dehalogenation obtained with zerovalent iron are partly due to the abundance of the nonreactive sorption and also due to the presence of the oxide layer acting as an additional barrier for electron transfer. It is not yet clear what exactly are the reactive sites. We hypothesized that the defects/abnormalities present on the surface of iron contribute to the reactive sites. The basis for this hypothesis lies in the corrosion literature. Review of the same indicated that these defects cause increased dissolution of the metal in the corrosion process, due to the phenomenon called localized corrosion.

Chloride pretreatment was used to increase the number of defects on the iron surface. This has two advantages. First, it is widely accepted in the literature that pitting is normally initiated by the aggressive anions such as halide ions. Since pitting corrosion is greatly enhanced by chloride ions,[32] it is possible that the dechlorination might favor further degradation if enough chloride accumulates. Thus, the reaction can act as an autocatalytic process. Second, in the presence of halide ions, the passive oxide layers formed on the surface of iron are known to break apart. At least two studies so far have indicated the presence of such an effect.[15,33] However, due to very small concentrations of the chloride ions present in the solutions, such autocatalytic effects are not evident in the reaction times studied so far. Moreover, though the driving force for reaction is corrosion of the metal, increasing the corrosion did not necessarily increase the degradation rate due to the competing water dissociation reaction.[12] Therefore, the corrosion process that was important for the dechlorination process was thought to be different in nature.

In this paper, we explore the possibility of induced pitting on the surface of iron as one of the techniques to improve the rates of the degradation process. The phenomenon of pitting corrosion is also seen in the scanning electron micrographs of iron samples observed over longer reaction times. To corroborate this further, iron was pretreated with chloride ions to introduce defects on the surface, and its effect on the TCE degradation rate was analyzed. These defects/pits present on the iron surface were found to be the controlling factor in determining the rate of reductive dehalogenation. We find that increasing the number of these surface abnormalities increases the rates considerably. Thus, the fractional active site concentration, as given by eq 2, is attributed to the number of defects/pits present on the surface of iron. The following section outlines the detailed experimental procedure adopted for the studies.

3. Experimental Section

3.1. Pretreatment of Iron. The electrolytic iron obtained from Fisher Scientific (100 mesh, 150 μm) was first treated with 1 M NaCl solution. Before treatment, the brine solution was heated to 100 °C, as the enhanced pitting is reported at higher temperatures.[34] Various other factors such as chloride concentration, pH of the solution, etc. influence the morphology of pits formed. Lower pH values have been found to give consistently higher pit formation even in the presence of small chloride concentrations. In the current approach, no attempt was made to treat the iron at lower pH, since at such low values loss of iron through dissolution would also be increased. To increase pit

(31) Gotpagar, J. Reductive Dehalogenation of Trichloroethylene (TCE) with Zerovalent Iron: Reaction Mechanisms and Transport Modeling. Ph.D. Dissertation, University of Kentucky, 1998.

(32) Bardwell, J. A.; Fraser, J. W.; MacDugall, B.; Graham, M. J. *J. Electrochem. Soc.* **1992**, *139*, 366.

(33) Johnson, T. L.; Fish, W.; Gorby, Y. A.; Tratnyek, P. G. *J. Contam. Hydrol.* **1998**, *29*, 379.

(34) Sato, N. *Corrosion* **1989**, *45*, 354.

formation, higher chloride concentration (1 M) was used and the iron samples were treated for 5 days.

The iron samples were washed with deoxygenated, deionized water for 3−4 cycles to remove the traces of chloride on the surface. This is a conservative approach because the presence of this species on the surface would have a benign effect (autocatalytic) if any. The samples were then immediately soaked in TCE solutions of known concentration, and placed on the rotary shaker at 5 rpm. At selected times, the aqueous samples were analyzed for TCE. The Hewlett-Packard 5890 Series II gas chromatograph, with an attached MS 5971A quadruple mass detector, was used for TCE analysis using a fused capillary column, J&W Scientific, DB-624. The analytical method followed the EPA method 624, with the following temperature program: oven temperature of 35 °C (4 min) to 200 °C at 6 °C/min, hold at 200 °C for 4 min. The carrier gas was zero-grade (high-purity) helium with a flow rate of 7.5 mL/min, and the MS scan range was $m/z = 35-260$ at 0.6 s/scan.

The chloride-treated iron samples were further characterized using SEM, surface profilometry, and AFM techniques. Initial AFM scans on Fisher electrolytic iron (100 mesh) showed that the AFM tip always moves the iron grains. To prevent this, the iron granules were embedded in a matrix of polyethylene (LDPE). This approach was also unsuccessful because of movement of grains. Therefore, iron chips were used in a separate experiment to be analyzable by AFM. The chips (35 × 10 × 3 mm) were obtained from hot rolled steel manufactured by Harbor Steel Corp., Lexington, KY. The experimental procedure followed for degradation studies was the same as that with Fisher iron.

3.2. Scanning Electron Microscopy. SEM provides an effective method for the characterization of the surfaces of samples. A narrow beam of electrons with kinetic energy in the range of 0−25 kV is incident on the iron surface. The sample was glued to the sample holder with colloidal graphite. The scanning electron microscope was a S-2300 model from Hitachi, and the images were recorded with 3000× magnification.

3.3. Surface Profilometric Studies. The surface profilometry studies were performed using a WYKO NT-2000 scanning white light interoferometry profiler. The WYKO is a noncontact optical device capable of measuring surface heights between 4 Å and 1 mm. Smooth surfaces can be measured in the phase-shifting interferometry (PSI) mode, while vertical-scanning interferometry (VSI) allows the measurement of rough surfaces and steps, without resorting to phase-unwrapping algorithms. In our studies we used the VSI mode to study the surfaces of treated/untreated iron.

3.4. Atomic Force Microscopy. A Park Autoprobe M5 atomic force microscope was used to profile the surface of treated/untreated samples of the iron chips before and after the chloride treatment. The atomic force microscope probes the surface of a sample with a sharp tip three μm long and 20 nm in diameter located at the free end of a cantilever. Forces between the tip and the sample surface cause the cantilever to bend and deflect. A laser beam reflected from the cantilever hits a detector area. The detector measures the current, proportional to the cantilever deflection, as the tip is scanned over the sample. These current measurements allow a computer to generate an image of surface topography. There are two main modes in operating an atomic force microscope: contact mode and noncontact mode. In the noncontact mode, the cantilever vibrates on the order of tens to hundreds of angstroms above the sample surface, and the interatomic force between the cantilever and sample is attractive. In the contact mode, the cantilever is held a few angstroms above the sample surface, and the interatomic force between the cantilever and the sample is repulsive. Since available iron chips have a homogeneous surface, we selected the contact mode for our studies.

The silicon tips attached to a cantilever with a low spring constant were used. The magnitude of the net force exerted to the sample varied from 8 to 15 nN (nanoNewtons). The scan speed was 100 mm/s. Typically a 100 mm × 100 mm field is scanned. Two morphologies were observed on the surface of untreated iron chips. A shiny (highly reflective) area represents the layers of the iron oxide. Dark areas (weak reflectivity) are associated with naturally occurring rust. On treated iron chips, a third morphology was observed. This was a grainy structure of iron that becomes apparent after the layer of iron oxide is removed.

4. Results and Discussion

4.1. Localized/Pitting Corrosion. Pitting is normally initiated by the aggressive anions such as halide ions. Several studies exist in the literature which talk about the mechanism of breakdown of passive films present on the surface of iron in the presence of chloride-containing media.[35,36] The breakdown requires a minimum amount of electrocapillary energy, whatever the mechanism of breakdown. Furthermore, the kinetic data of Pou et al.[36] reveal that the breakdown of oxide layers was consistent with the ion exchange processes, point-defect models, and hydrated polymeric oxide model. For a review of the mechanistic aspects of the breakdown of oxide layers, the reader is referred to the above two references. In this paper, only results pertaining to our studies will be explained.

At this point, it is instructive to examine the SEM photographs of the iron (Fisher iron) samples obtained after TCE degradation. Parts a and b of Figure 2 show the scanning electron micrographs of the fresh iron surface and the iron surface after 81 h of degradation of TCE, respectively. The effect of localized corrosion is not very evident from these photographs. Figure 2c shows SEM of the iron surface after 120 days of reaction time. It can be seen that the localized corrosion is much more pronounced after longer reaction times. This indicates the breakdown of the precipitates with chloride ions. This is also consistent with the result of Helland et al.,[15] who reported a 60% increase in the CCl_4 dechlorination rates with increased contact time, for the specific case of batch systems with zerovalent iron. Thus, this can be interpreted as an autocatalytic effect observed due to pitting corrosion in the presence of chloride ions generated as a product of reaction. As can be seen from Figure 2c, the corrosion indeed appears to be localized and can be termed as crevice corrosion.

It is quite clear that chloride ions are responsible for the crevice corrosion observed. Therefore, we hypothesize that increasing this form of corrosion should increase the degradation rates. To investigate this, we deliberately treated the iron surface with chloride ions prior to its exposure to TCE solution. The morphological changes expected due to the attack of chloride ions are defects on the surface with trenches and peaks. The effect of this surface modification on the TCE degradation has been outlined in the subsequent sections.

4.2. Effect of Surface Pretreatment on TCE Degradation. Figure 3 shows the results of TCE degradation profiles obtained after the chloride treatment of Fisher electrolytic iron (100 mesh). The results obtained with untreated iron are also compared in the figure. These results show that TCE degradation is indeed increased by the chloride treatment. This increase is most prominent in the reaction at early times. At later times, the effect of chloride pretreatment provides little improvement (not shown). Figure 3 shows the pronounced effect of chloride treatment on the TCE degradation. This is also evident from Figure 4, where the pseudo-first-order rate constants for the degradation are plotted on the basis of the initial rates. As can be seen from the figure, chloride pretreatment provided almost 2-fold increase (from 0.019 to 0.037 h^{-1}) in the initial rate constant. Similar enhancements in the

(35) Sato, N. *J. Electrochem. Soc.* **1982**, *129*, 255.
(36) Pou, T. E.; Murphy, O. J.; Young, V.; Bockris, J. *J. Electrochem. Soc.* **1984**, *131*, 1243.

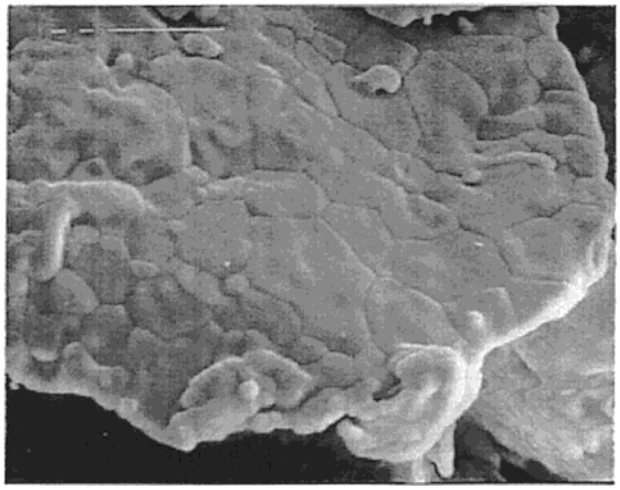

(a)

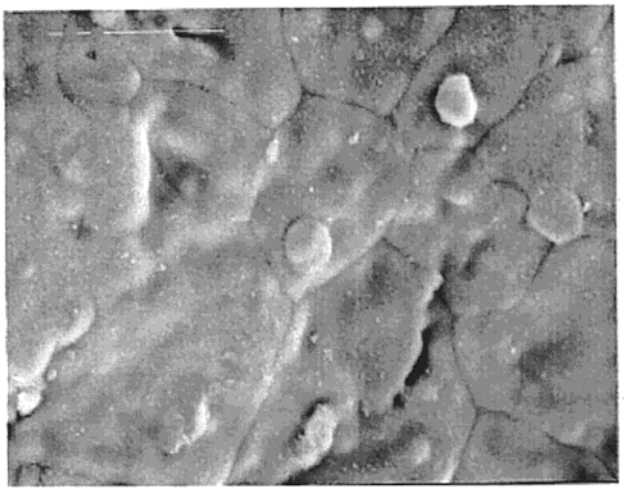

(b)

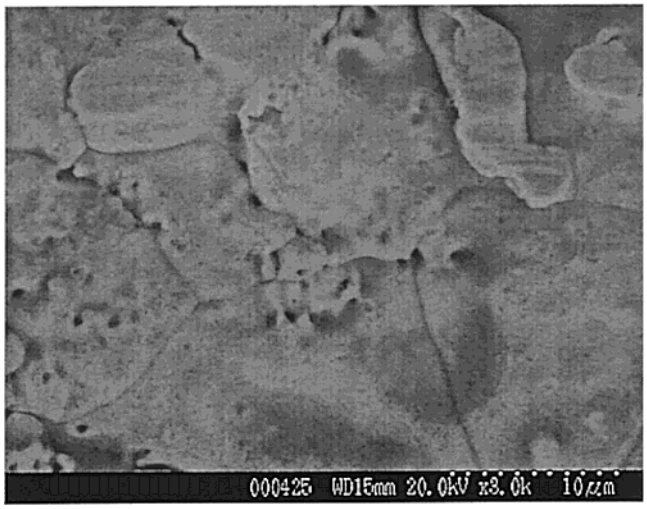

(c)

Figure 2. Evidence of crevice corrosion. SEM photographs of the iron surface: (a) fresh iron surface; (b) iron surface after 81 h of reaction; (c) iron surface after 120 days of reaction time.

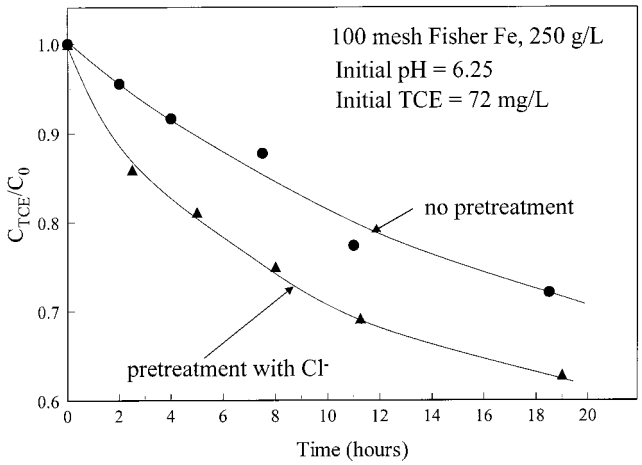

Figure 3. Effect of chloride treatment on the TCE degradation: (a) overall degradation profile; (b) enhancement in the initial degradation rates.

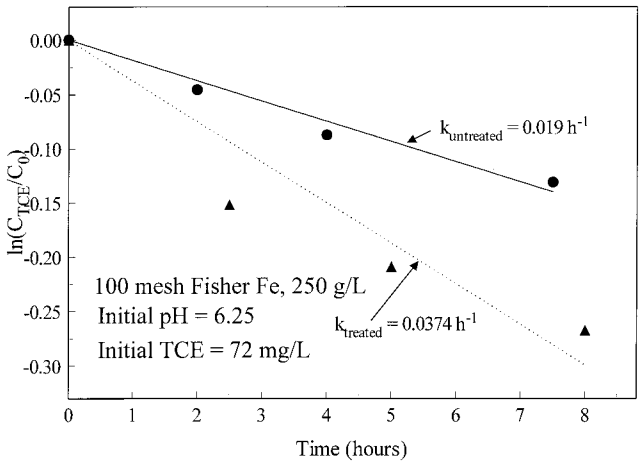

Figure 4. Effect of chloride treatment on the initial TCE degradation rate constant.

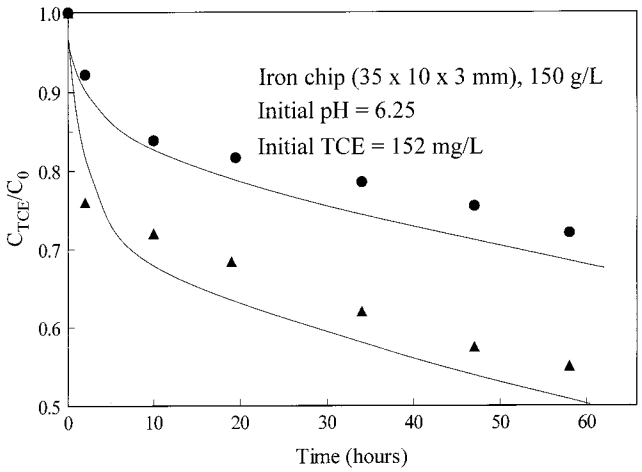

Figure 5. Effect of chloride treatment on TCE degradation with iron chips.

TCE degradation rates are also observed for iron chips from chloride pretreatment (Figure 5). As can be seen from Figure 5, the initial rates were again enhanced by the chloride treatment. It should be noted that the iron chips used in this study have very low external surface area, resulting in the low degradation rates. However, even with such low surface areas, the effect of chloride treatment is quite evident. Comparison of Figures 3 and

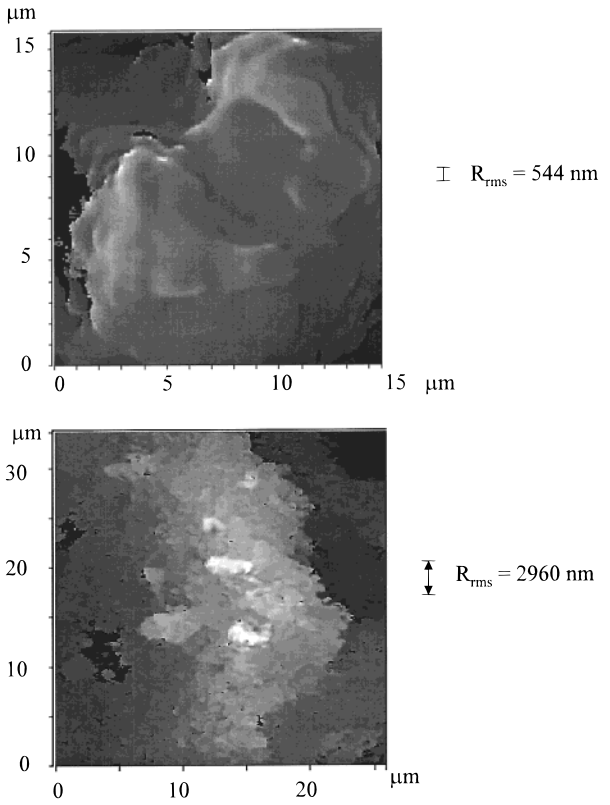

Figure 6. Surface profilometric data on the iron surface: (a, top) fresh iron surface; (b, bottom) iron surface after chloride treatment.

5 also reveals that the initial decline obtained with iron chips is much faster than that with 100 mesh Fisher iron fillings. The reason for this is not clear, although it is possible that even though iron chips have lower external surface areas, the additional internal surface area created by crack formation after the pretreatment might be more than that for the 100 mesh iron filings.

4.3. Surface Profilometric Results. Gray-scale renditions (obtained using the WYKO) of the surface topography for the fresh iron and chloride-treated iron are shown in Figure 6. These images show that the chloride-treated surface is much more rough than the untreated surface. This can be quantified by calculating the standard deviation of the 2D surface profile. The root-mean-square roughness for the untreated sample is 544 nm, and that for the treated sample is 2960 nm, which is 5.4 times greater than that of the untreated sample. This is also evident from the height variation along the *x* and *y* coordinate directions, as depicted in Figure 7. The fresh iron surface, i.e., covered with oxide, does have some variation (not shown) or, in other words, defects on the surface. We hypothesized that these defects are indeed the places where reaction takes place. In other words, the active sites[17,30] where the reactive sorption is assumed to occur are these defects or cracks on the surface. Attempts to increase this number of cracks by chloride pretreatment indeed resulted in the increase in the reaction. This further corroborates our hypothesis, which is also clear from Figure 7. To check whether increased roughness is actually due to the presence of chloride, iron was also treated in deionized water for 5 days in the absence of chloride. Comparison of the surface plot of corroded iron in the presence and absence of chloride (not shown) revealed that the roughness observed on the surface indeed was due to the pitting effect produced by chloride treatment.

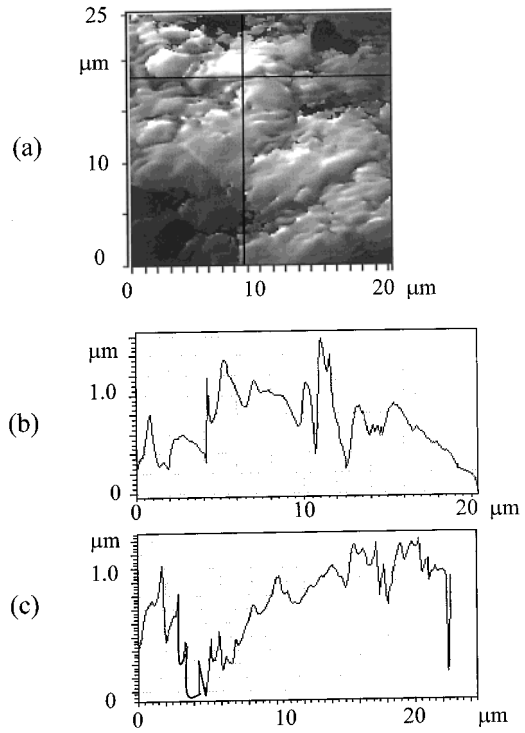

Figure 7. Surface profilometric data on the iron surface after 5 days of chloride pretreatment: (a) surface image; (b) vertical profile of surface roughness; (c) horizontal profile of surface roughness.

The effect of this surface treatment is reflected in the increase in the degradation rates, which is shown in Figures 3−5. Thus, our hypothesis that such a surface roughness is beneficial for TCE degradation seems to be justified. Furthermore, the decline in the enhancement at longer times can be explained with the help of Figure 8. Examination of Figure 8 shows that though the iron surface after reaction appears rough at first glance, the height variations (peaks/valleys) on the surface have diminished compared to those on the freshly treated iron surface. As a result, there is no more rate enhancement because of reduction in the number of active sites (defects/pits) available as hypothesized earlier. The average roughness was found to be considerably less for the sample after 60 h of reaction, indicating that pits initially present are either being filled over the course of reaction or are being eaten away due to reaction, leaving a smoother metal surface as found by Boronina et al.[8] in the case of zinc. The possible reasons for this again can be formation of precipitates. Carrying out the reaction in chloride-containing media would therefore have a benign effect as found by other researchers. Roberts and Fennelly[23] showed that the presence of high Cl^- during the 1,1-TCA reduction reaction prevents the repassivation of the iron surface. On the other hand, in the elegant work of Li and Klabunde,[25] bimetallic systems were found to enhance the overall degradation rate.

4.4. AFM Images. AFM studies were undertaken to characterize the three-dimensional changes on the morphology of the iron surface with the chloride treatment and the reaction, to better visualize the defects present on the iron surface. The images shown here are only with the iron chips (TCE degradation results shown in Figure 5).

Figure 9 gives the AFM images for the fresh iron chip and the chloride-treated iron chip. The figure indicates that the surface features observed with the surface profilometer can be better viewed with AFM images. No

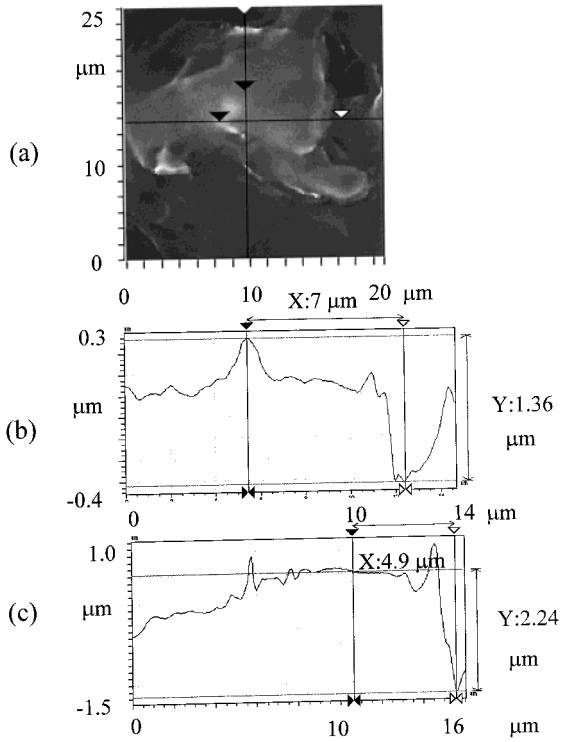

Figure 8. Surface profilometric data on the iron surface after 60 h of reaction: (a) surface image; (b) vertical profile of decreased surface roughness; (c) horizontal profile of decreased surface roughness.

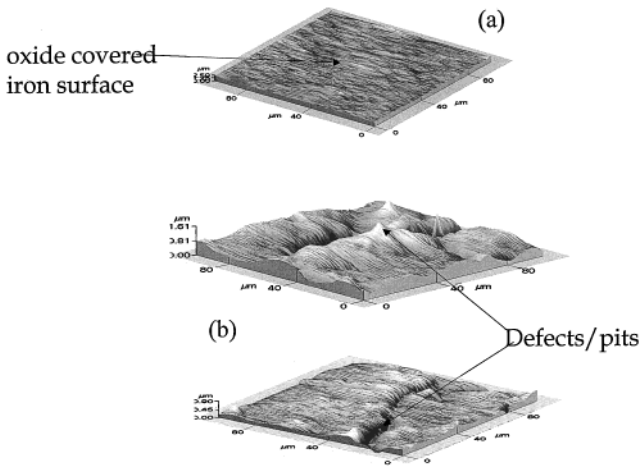

Figure 9. AFM images: (a) oxide-covered iron chip; (b) chloride-treated iron chip.

special features were observed on the oxide-covered iron surface, other than occasional dark and shiny areas as mentioned earlier. This is shown in Figure 9a. Figure 9b clearly shows the evidence of the enhanced corrosion along grain boundaries of iron as a result of the chloride treatment. We further studied the defects/abnormalities present on the surface. This is shown with the help of a two-dimensional view of the chloride-treated sample (Figure 9b), in Figure 10. It was found that the typical depth of the trenches varied from 0.1 to 0.5 μm, and the width of the trenches between the grains of iron varied from 11 to 16 μm. This is presented in Figure 10 through three profiles of a trench located between two grains of iron on the surface of the treated chip.

The effect of these surface defects and pits on the iron chips on the TCE degradation profiles is shown in Figure 5. It should be noted that the iron chips used in this study

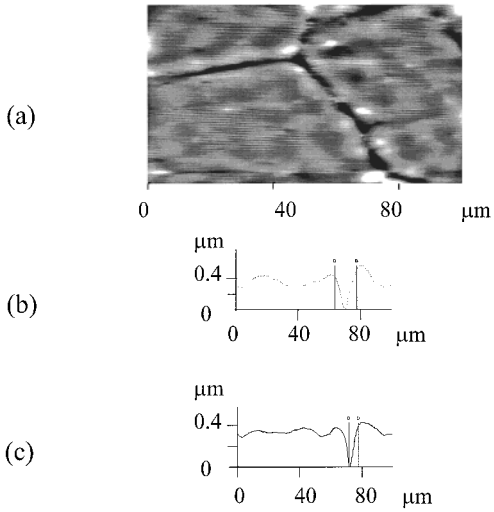

Figure 10. (a) 2-D representation of Figure 8. (b, c) Vertical profiles of trenches.

were obtained from scrap metal inventory and therefore have an oxide layer. As a result, the active external surface area of the metal is very low. Nonetheless, even with such low surface areas, the enhanced dechlorination due to defects on the surface of iron is evident from Figure 5. This again confirms the hypothesis of the defects being active sites, mainly responsible for TCE degradation.

It should be noted that the surface abnormalities can be enormously increased by varying the treatment conditions.[34,35] A systematic study of these conditions will be required to achieve the optimum treatment condition, which can yield much higher degradation rates than that observed in the present study. One can also see that, as the reaction proceeds, these surface deformities diminish (Figure 8). This explains the possible reasons for the decrease in the reaction rates at longer times. However, in the presence of externally added chloride, one can enforce these deformities on the surface by continuous breakdown of the oxide precipitates that might be formed. This was confirmed by a recently published study,[23] in which much higher degradation rates of dechlorination of 1,1,1-TCA with Fe^0 in the presence of 0.1M NaCl in the reaction system were observed. Another study[33] also found that the addition of chloride ion increased the rate of CCl_4 dechlorination as high as 4-fold.

5. Possible Mechanisms for Observed Enhancement

Until now we have discussed the evidence observed for the pitting corrosion during the reductive dehalogenation of TCE with zerovalent iron. The evidence of this corrosion mechanism was further corroborated by the observed enhancements obtained by creating more pits. In this section, an attempt is made to explain the reason for this by making use of the corrosion literature.

In a recently published study, Scherer et al.,[37] have given an excellent review of the different roles that oxide layers present on the surface of iron might play during the reductive dehalogenation reaction. To explain the current results, we have used the concept of the role of the oxide layer as a physical barrier, as explained in this paper. We observed pit formation through these oxide layers when

(37) Scherer, M. M.; Balko, B. A.; Tratnyek, P. G. The Role of Oxides in Reduction Reactions at the Metal-Water Interface. In *Kinetics and Mechanisms of Reactions at the Mineral/Water Interface*; Sparks, D. L., Grundl, T., Eds.; ACS Symposium Series; American Chemical Society: Washington, DC, 1998.

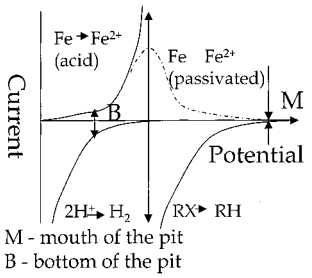

Figure 11. Possible mechanism for the observed enhancement in dechlorination rates (adapted from ref 37).

the iron was pretreated with chloride-containing solution. It should be noted that these pits create new, longer diffusion paths[35,38−40] for TCE to react with the bare metal at the bottom of the pit. Such longer diffusion paths to the bottom of the pit restrict the transport of aqueous species from the bulk of the solution. These longer diffusion paths might lower the degradation rates of TCE. However, it should be noted that two additional phenomena are encountered[37] due to pit formation. First, anodic metal dissolution in aqueous solutions containing Cl^- ion generally leads to the accumulation of metal ions and chloride ions adjacent to the metal surface. In the case of iron group metals, the accumulation of metal ions gives rise to acidification due to metal ion hydrolysis. On the other hand, relatively alkaline conditions exist at the mouth of the pit, which may favor repassivation of the surface due to Fe^{2+} diffusing from below. As with the case of crevice corrosion of iron in the presence of chloride ions, the overall rate of the process can be enhanced through the formation of surface defects, or pits.

Macroscopically, pit breakdown can be described by the current (i)−potential (E) curve. An example of a $i-E$ curve is shown in Figure 11.[37] The two half-reactions completing the electrochemical cell in both the bottom and mouth of the pit are also shown in Figure 11. As mentioned before, the conditions at the bottom of the pit are more acidic, and the half-reaction of dissolution of iron is primarily balanced by the reduction of water (because of restriction of TCE to approach the bottom of the pit due to induced longer paths). At the mouth of the pit, the half-reactions are dissolution at a passivated iron metal surface (alkaline conditions) and possible reduction of water or stronger oxidants such as oxygen or TCE. Thus, the conditions in the pit create two electrochemical cells, one at the bottom and other at the mouth of the pit. Whenever two electrochemical or galvanic cells are in close proximity to each other, the net corrosion rate of the metal is more than that with just one cell.[34] The enhancement in the degradation rate at early times could thus be attributed to the acceleration of corrosion associated with pitting results. This occurs because the close proximity of the two cells creates a coupled cell where acidic iron dissolution at the bottom of the pit and reduction of TCE at the mouth of the pit become the controlling anodic and cathodic processes. According to Scherer et al.,[37] the net rate of dehalogenation in this case would be equal to the rate of corrosion. Furthermore, the typical size of the pit observed was 11−16 μm. One of the factors governing stability of pits, or in other words preventing repassivation of pits, is the pit size. Sato[38] reports that the critical pitting radius required for stable pitting is 10−20 μm. The value we observed was also in this range, further supporting our claim about the stability of the pits. The imperfections of this order could act as initial sites for pitting.[35] The results obtained so far indicate that such a pitting mechanism seems to enhance the rate of dechlorination of TCE. In such a scenario, the major half-reaction at the mouth of the pit (in the absence of the oxygen) would be the dehalogenation of TCE. This possibility has also been speculated in a recent paper.[37]

There is, however, one more possibility for the observed enhancement. Pitting dissolution, as discussed earlier, leads to evolution of the hydrogen gas at the bottom of the pit. The possibility of this hydrogen acting as a direct reducing agent has already been discussed by Matheson and Tratnyek.[3] However, to have such action, catalysts are required. Matheson and Tratnyek[3] point out the possibility of defects/pits present on the surface acting as catalysts for such direct hydrogenation. In this study, as evidenced by AFM images and surface profilometric data, defect and pit formation was increased by chloride treatment. These defects could thus act as catalysts for the direct reduction by hydrogen generated as a result of corrosion, leading to enhancement in the reaction rate.

There is a need to do more research in this area to discern the exact mechanism responsible for the observed enhancement.

6. Conclusions

Surface characterization techniques have been employed to gain insight into the metallic surface effects involved in the reductive dehalogenation of TCE with zerovalent iron. It has been found that the defects present on the surface act as reactive sites for the dehalogenation process. A simple way to increase the number of abnormalities on the surface is by chloride pretreatment, and thus causes improvement in the degradation rates at early times. But these enhancements disappear at longer reaction times, which is attributed to the decrease in the surface roughness over the course of reaction. The increased reaction rates were attributed to the morphological changes occurring on the surface of iron, which were studied using surface profilometry and AFM. Two possible mechanisms, the proximity of two electrochemical cells and the direct hydrogenation in the presence of defects acting as catalysts have been proposed. This research explores a new approach for surface modifications that can enhance the degradation rates. Moreover, such surface modifications can also lead to reduced remediation times in in situ applications. Further analysis of the correlation between the surface defects and the degradation rates with the goal of determining optimum conditions needs to be investigated.

Acknowledgment. This study was partially supported by a Memorandum of Agreement between the Kentucky Natural Resources and Environmental Protection Cabinet and the University of Kentucky through the Kentucky Water Resources Research Institute. S.L. and R.C. acknowledge the support of NASA cooperative agreement NCC5-222, ONR Grant N00014-96-1296, and NSF Grant ECS-9724371.

Nomenclature

A_S	fractional active site concentration
b	Langmuir adsorption isotherm parameter
C^S_{TCE}	total concentration of TCE on the iron surface [nmol/g]

(38) Sato, N. *J. Electrochem. Soc.* **1982**, *129*, 260.
(39) Hassan, S. M.; Wolfe, N. L.; Cipollone, M. G.; Burris, D. R. *Prepr. Extended Abstr. Am. Chem. Soc.* **1993**, *33*.
(40) Roberts, A. L.; Totten, L. A.; Arnold, W. A.; Burris, D. R.; Campbell, T. J. *Environ. Sci. Technol.* **1996**, *30*, 2654.

C_{TCE}^{S*} concentration of TCE on the iron surface at the active sites [nmol/g]

C_{TCE}^{W} concentration of TCE in the aqueous phase [nmol/ml]

k Lagmuir adsorption isotherm parameter

$k_{intrinsic}$ intrinsic value of the degradation constant of TCE with zerovalent iron [h^{-1}]

k_{obs} observed value of the degradation constant [h^{-1}]

M Langmuir adsorption isotherm parameter

m_{Fe} amount of iron used in the reaction system [g]

V_W volume of the aqueous phase [L]

LA990325X